JACS
JOURNAL OF THE AMERICAN CHEMICAL SOCIETY
Article
pubs.acs.org/JACS

Copolythiophene-Derived Colorimetric and Fluorometric Sensor for Visually Supersensitive Determination of Lipopolysaccharide

Minhuan Lan,[†,§] Jiasheng Wu,[†] Weimin Liu,[†] Wenjun Zhang,*[,‡] Jiechao Ge,[†] Hongyan Zhang,[†] Jiayu Sun,[†,§] Wenwen Zhao,[†,§] and Pengfei Wang*[,†]

[†]Key Laboratory of Photochemical Conversion and Optoelectronic Materials, Technical Institute of Physics and Chemistry, Chinese Academy of Sciences, Beijing, 100190, People's Republic of China

[‡]Center of Super-Diamond and Advanced Films (COSDAF) and Department of Physics and Materials Science, City University of Hong Kong, Hong Kong SAR, P.R. China

[§]Graduate School of the Chinese Academy of Sciences, Beijing, 100049, China

Supporting Information

ABSTRACT: 3-Phenylthiophene-based water-soluble copolythiophenes (CPT**1**) were designed for colorimetric and fluorometric detection of lipopolysaccharide (LPS). The sensor (CPT**1**-C) shows a high selectivity to LPS in the presence of other negatively charged bioanalytes as well an extreme sensitivity with the detection limit at picomolar level, which is the lowest ever achieved among all synthetic LPS sensors available thus far. Significantly, the sensing interaction can be apparently observed by the naked eyes, which presents a great advantage for its practical applications. The appealing performance of sensor was demonstrated to originate from the multiple electrostatic and hydrophobic cooperative interactions, synergetic with signal amplification via the conformational change of the 3-phenylthiophene-based copolymer main chain. As a straightforward application, CPT**1**-C is capable of rapidly discriminating the Gram-negative bacteria (with LPS in the membrane) from Gram-positive bacteria (without LPS).

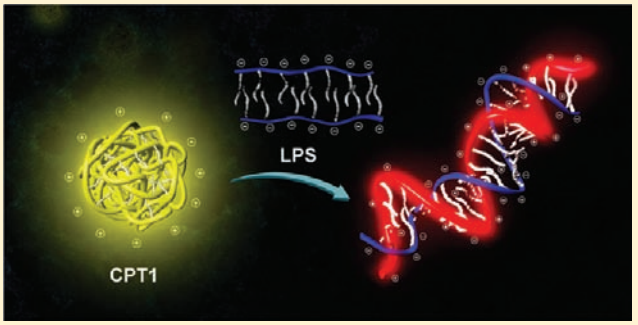

INTRODUCTION

Lipopolysaccharide (LPS) is a structural component in the outer cell membranes of all Gram-negative bacteria (also named endotoxin).[1] LPS is highly toxic and biologically active even at a concentration as low as pg/mL range.[2] Sepsis and septic shocks, arising from the massive release of LPS, cause about 150 000 casualties annually in the United States.[3] Due to its high toxicity at a low concentration, the specific and sensitive determination of LPS is of a particular interest. Currently, enzymatic limulus amebocyte lysate (LAL) assay is clinically used for the determination of endotoxin via the gel formation between LAL and endotoxin.[4] However, the LAL assay is highly susceptible to changes in temperature and pH. Moreover, carbohydrate derivatives other than LPS, such as β-glucans, also respond positively to LAL. Thus, many efforts have been devoted to develop highly sensitive and selective sensors for LPS detection in the recent years.[5−8] For instance, Basu et al. reported a colorimetric sensor for LPS based on functionalized polydiacetylene liposome,[5] which could function at a high LPS concentration above 100 μM. Brock et al. developed a FRET-based sensor consisting of a CD14-derived LPS-binding peptide terminally labeled with organic fluorophores that can detect LPS at a concentration of micromolar range.[6] Very recently, Carsten Schmuck et al. reported a peptide-functionalized polydiacetylene liposome acting as a fluorescent turn-on sensor for LPS.[7] Although the detection sensitivity for LPS has been improved from millimolar to submicromolar level thus far, it is still a great challenge to meet the requirement to detect LPS at toxic concentration of picomolar level.

In recent years, water-soluble conjugated polythiophenes with charged substituents and steroidal groups for sensing biological relevant targets, such as DNA, proteins, ATP, and folic acid have received considerable attention.[9−11] The homopolythiophene-based sensors generally show good sensitivity due to amplification by a collective system response, and thus offer a great superiority over the sensors based on small molecules.[12] However, they often display a low selectivity to analytes,[13] and show single signal response to binding events, as a result, sensing may be affected by some uncertain factors such as the instrumental efficiency, environment condition, and molecular concentration.[14]

Along with our continuing efforts in the exploration of fluorescent chemsensors for bioactive molecules including LPS, heparin and antibiotics,[15] we herein employ a new design strategy by means of copolymerization of 3-phenylthiophene

Received: December 11, 2011
Published: March 27, 2012

   dx.doi.org/10.1021/ja211570a | J. Am. Chem. Soc. 2012, 134, 6685−6694

Scheme 1. Synthetic Routes of CPT1-A, CPT1-B, and CPT1-C and Model Polymers PT1 and PT2

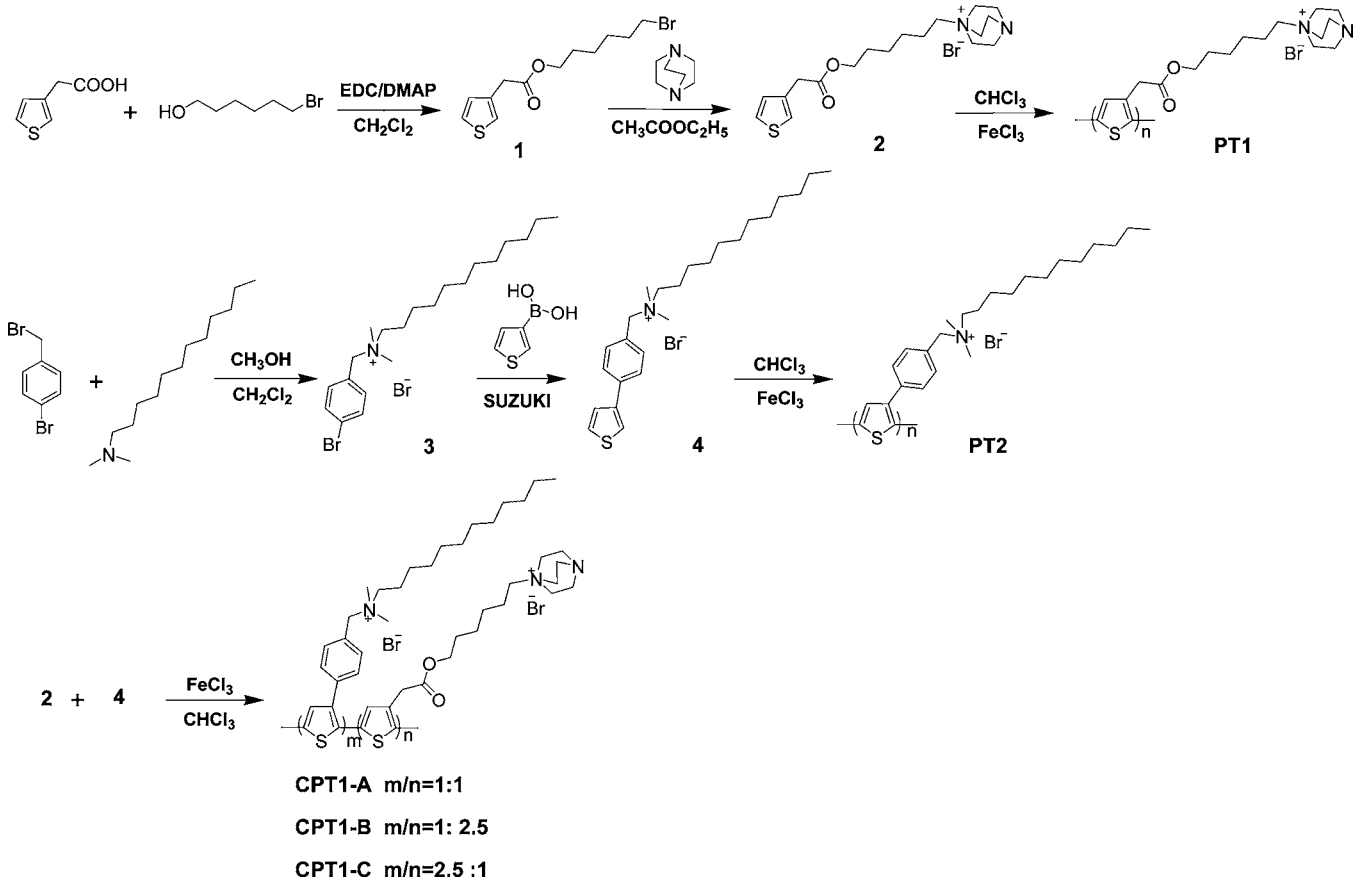

bearing quaternary ammonium and DABCO group substituted thiophene to overcome the above setbacks. The phenyl as a rigid group is attached to the 3-position of thiophene to tune the conformation of copolymer chain, resulting in the signal amplification;[12] and DABCO moiety is introduced by means of its strong affinity to phosphate groups in LPS.[16] This appealing sensing platform is expected to show the following advantages: i) good stability and water solubility, ii) multiple electrostatic and hydrophobic cooperative interactions for highly selective detection toward LPS, iii) high signal-to-noise ratio and the capacity for signal amplification, and iv) significant red-shift in both the absorption and fluorescence wavelength upon interaction with LPS. This approach enables us to design new colorimetric and fluorometric sensors for LPS with high selectivity and a detection limit down to the picomolar level. Furthermore, this design strategy is straightforwardly adaptable to a variety of sensors for highly sensitive and selective detection of various biologically important polyanions by introducing different polymerized units and recognized groups. To illustrate the importance of copolymerization applied in our design for highly selective and sensitive determination of LPS, two corresponding homopolymers (PT**1** and PT**2**) were also synthesized as model polymers (Scheme 1). The results show that neither PT**1** nor PT**2** display decent signal responses to LPS because of the lack of cooperative interactions as shown by CPT**1**-C.

EXPERIMENTAL SECTION

General Materials and Methods. All UV−vis and fluorescence spectra in this work were recorded in Hitachi U3010 and Hitachi F-4500 fluorescence spectrometers. The water was purified by Millipore filtration system. ^{1}H NMR (400 MHz) and ^{13}C NMR (100 MHz) spectra were collected on a Bruker Advance-400 spectrometer with tetramethylsilane as an internal standard. Electron impact (EI) mass spectroscopy was carried out on a Waters GCT Premier mass spectrometer. Matrix-assisted laser desorption ionization-time-of-flight (MALDI-TOF) mass spectra were obtained on a Bruker Microflex mass spectrometer and electrospray ionization (ESI) mass spectra on a Shimadzu LC-MS 2010 instrument. The gel-permeation chromatography was performed using gelatin as the standard, and the CH_3CN−water mixture solution containing $NaNO_3$ (0.2 M) and CH_3COOH (0.5 M) under pH 5 was employed as eluent. Transmission electron microscopy (TEM) images were taken on a JEOL JEM-2100F operated at an acceleration voltage of 150 kV. Atomic force microscopy (AFM) measurements were conducted using the DI Multimode SPM from Veeco Systems and the images were obtained with the tapping mode. Zeta potentials were recorded on Zetasize 3000 HS (Malvern, UK). Dynamic light scattering was performed on Dybapro Nanostar from Wyatt Technology Corporation.

4-Bromobenzyl bromide, *N*,*N*-dimethyldodecylamine, thiophene-3-boronic acid, tetrakis(triphenylphosphine)palladium(0), 3-thiopheneacetic acid, 6-bromo-1-hexanol, 4-(dimethylamino)pyridine, 1-(3-dimethylaminopropyl)-3-ethylcarbodiimide hydrochloride, and 1,4-diazabicyclo[2.2.2]octane were purchased form Alfa Aesar. ctDNA, RNA, γ-globulins, NAD^+, adenosine, AMP, ADP, ATP, guanine, adenine, glucose, BSA, phosphatidylcholine, LPA, lipid A, EDTA, malic acid, citric acid, chondroitin 4-sulfate sodium salt, heparin, hyaluronic acid, and acetate were purchased from Sigma. Lipopolysaccharide (LPS) was purchased from Sigma, which was obtained from *Escherichia coli* 055:B5. Note that the molecular weight of commercial LPS varies between 3 and 20 KDa, and we assume a molecular weight of 10 KDa in this work. Lipoteichoic acid (LTA), obtained from *Staphylococcus aureus*, was purchased from Sigma. Other reagents were purchased from Beijing Chemical Regent Co. All

dx.doi.org/10.1021/ja211570a | J. Am. Chem. Soc. 2012, 134, 6685−6694

reagents and chemicals were AR grade and used without further purification unless otherwise noted. CH_2Cl_2 and $CHCl_3$ were distilled from CaH_2 under nitrogen. *Escherichia coli* ATCC 25922, *S. aureus* ATCC 6538, *Staphylococcus epidermidis* ATCC 12228, *Klebsiella pneumoniae* AS1.1736, and *Pseudomonas aeruginosa* AS1.2031 were purchased from Antibacterial Material Testing Center of Technique Institute of Physics and Chemistry, Chinese Academy of Sciences.

Syntheses of Sensor Probes and Model Polymers. The synthetic routes of CPT**1**-A, CPT**1**-B, CPT**1**-C, and model polymers PT**1** and PT**2** were outlined in Scheme 1, and the details were described below.

6-Bromohexyl-2-(thiophen-3-yl)acetate (Compound 1). 6-bromo-1-hexanol (0.362 g, 2 mmol) was added slowly with syringe to a mixture of 1-(3-dimethylaminopropyl)-3-ethylcarbodiimide hydrochloride (0.5 g, 2.6 mmol), 4-(dimethylamino)pyridine (70 mg, 0.6 mmol) and 3-thiopheneacetic acid (0.284 g 2 mmol) in 40 mL of dry CH_2Cl_2 under nitrogen. The mixture was stirred at room temperature for 12 h to complete the reaction. The solution was washed with H_2O (3×20 mL) and the organic layer was dried with anhydrous $MgSO_4$. After removal of the solvent under reduced pressure, the residue was purified by column chromatography (eluent: petroleum ether/ethyl acetate = 5:1) to give compound **1** (0.45 g, yield 74%) as a colorless liquid. ^{1}H NMR (400 MHz, $CDCl_3$, TMS, ppm): δ 1.34−1.36 (m, 2H), 1.43−1.46 (m, 2H), 1.60−1.66 (m, 2H), 1.83−1.86 (m, 2H), 3.37−3.41 (t, J = 13 Hz, 2H), 3.65 (s, 2H), 4.09−4.12 (t, J = 13 Hz, 2H), 7.03−7.05 (d, J = 6 Hz, 1H), 7.14−7.15 (t, 1H), 7.26−7.29 (m, J = 13 Hz, 1H). ^{13}C NMR (100 MHz, $CDCl_3$, TMS, ppm): δ 25.1, 27.8, 28.5, 32.6, 33.7, 36.0, 64.8, 122.8, 125.7, 128.5, 133.8, 171.2. EI Mass spectrum m/z: Calculated: 306.01 (100%), 304.01 (98.2%); Found: 306.01, 304.01.

1-(6-(2-(Thiophen-3-yl)acetoxy)hexyl)-4-aza-1-azoniabicyclo[2.2.2]octane Bromide (Compound 2). 1,4-Diazabicyclo-[2.2.2]octane (0.2 g, 1.8 mmol) was dissolved in 50 mL of ethyl acetate with the subsequent addition of intermediate **1** (0.3 g, 1 mmol). The mixture was stirred at room temperature for 36 h to complete the reaction. The resulting white precipitation was collected, washed with ethyl acetate, and dried in vacuum to give compound **2** as a white solid (0.25 g, yield 60%). ^{1}H NMR (400 MHz, CD_3OD TMS, ppm): δ 1.35−1.46 (m, 4H), 1.64−1.70 (m, 2H), 1.71−1.77 (m, 2H), 3.18−3.25 (m, 8H), 3.30−3.36 (m, 6H), 3.67 (s, 2H), 4.11−4.14 (t, J = 13 Hz, 2H), 7.03−7.05 (d, J = 5 Hz, 1H), 7.22−7.23 (m, 1H), 7.36−7.38 (d, J = 8 Hz, 1H). ^{13}C NMR (100 MHz, CD_3OD, TMS, ppm): δ 22.7, 26.4, 26.9, 29.3, 36.4, 46.1, 53.4, 65.5, 65.7, 123.9, 126.7, 129.7, 135.4, 173.0. MALDI-TOF Mass spectrum m/z: Calculated: 337.19; Found: 337.03.

***N*-(4-Bromobenzyl)-*N*,*N*-dimethyldodecan-1-aminium Bromide (Compound 3).** 4-Bromobenzyl bromide (0.25 g, 1 mmol) was dissolved in 20 mL of CH_2Cl_2/CH_3OH (v/v = 3/2) with the subsequent addition of *N*,*N*-dimethyldodecylamine (0.4 mL, 1.3 mmol). The mixture was stirred at room temperature for 12 h. After the reaction was completed, the reaction solution was concentrated to 5 mL. The residue was poured into 200 mL of absolute diethyl ether under stirring and then filtered. The precipitate was filtered, washed with absolute diethyl ether and dried to give compound **3** (0.43 g, yield 92%) as a white solid. ^{1}H NMR (400 MHz, $CDCl_3$, TMS, ppm): δ 0.82−0.87 (t, 3H), 1.21−1.26 (m, 18H), 1.75 (m, 2H), 3.24−3.26 (s, 6H), 3.48−3.52 (m, 2H), 5.17−5.21 (s, 2H), 7.49−7.51(d, J = 8 Hz, 2H), 7.58−7.60 (d, J = 8 Hz, 2H). ^{13}C NMR (100 MHz, $CDCl_3$, TMS, ppm): δ 13.8, 22.4, 22.7, 26.1, 29.0, 29.1, 29.3, 31.6, 49.2, 63.7, 66.1, 125.2, 126.3, 132.1, 134.7. MALDI-TOF Mass spectrum m/z: Calculated: 382.21 (100%), 384.20 (97.4%); Found: 382.27, 384.29.

***N*,*N*-Dimethyl-*N*′-(4-(thiophen-3-yl)benzyl)dodecan-1-aminium Bromide (Compound 4).** Deionized water (10 mL) was added with syringes to a mixture of compound **3** (0.4 g, 0.86 mmol), Na_2CO_3 (0.5 g, 4.7 mmol), $Pd(PPh_3)_4$ (200 mg, 0.17 mmol), and thiophene-3-boronic acid (0.128 g, 1 mmol) in EtOH (20 mL) under nitrogen. After refluxing at 90 °C for 6 h, EtOH was removed under reduced pressure. The residue was extracted with CH_2Cl_2 (3×20 mL) and the resulting organic layer was collected and dried with anhydrous $MgSO_4$. After removal of the solvent under reduced pressure, the residue was purified by column chromatography (eluent: CH_2Cl_2/CH_3OH = 12:1) to give compound **4** (0.3 g, yield 75%) as a colorless solid. ^{1}H NMR (400 MHz, $CDCl_3$, TMS, ppm): δ 0.86−0.89 (t, 3H), 1.23−1.33 (m, 18H), 1.80 (m, 2H), 3.31 (s, 6H), 3.51−3.56 (m, 2H), 5.14 (s, 2H), 7.35−7.36 (d, J = 5 Hz, 1H), 7.39−7.41 (d, J = 8 Hz, 1H), 7.49 (s, 1H), 7.61−7.63 (d, J = 8 Hz, 2H), 7.69−7.70 (d, J = 8 Hz, 2H). ^{13}C NMR (100 MHz, $CDCl_3$, TMS, ppm): δ 14.1, 22.7, 23.0, 26.4, 29.3, 29.5, 29.6, 31.9, 49.6, 63.8, 67.2, 121.7, 126.0, 126.8, 126.9, 133.9, 137.9, 140.8. MALDI-TOF Mass spectrum m/z: Calculated: 386.29; Found: 386.13.

General Syntheses of Polythiophenes. All polymers in this paper were prepared via an oxidative polymerization under nitrogen in the presence of $FeCl_3$. The general method for preparation of polythiophenes was carried out as follows: 4 equiv of $FeCl_3$ was dissolved in 30 mL of dry $CHCl_3$ under nitrogen, and then 1 equiv of corresponding monomers dissolved in 20 mL of $CHCl_3$ was added dropwise. The reaction mixture was stirred at room temperature for 2 days. The resulting precipitate was collected, washed with methanol, and finally dried under vacuum to give the desired polymers as a dark red solid. For the copolymerization, monomer **4** and **2** with different mole ratios (1/1, 1/2.5, and 2.5/1) were used to give the corresponding copolythiophenes (CPT**1**-A, CPT**1**-B, and CPT**1**-C, respectively). The polymerization of monomer **2** and **4** gives the corresponding homopolythiophenes PT**1** and PT**2**, respectively.

CPT1-A (Yield: 22%) Gel-Permeation Chromatography Analysis (GPC). $M_n = 9.789 \times 10^4$, polydispersity index (PDI = 1.100) ^{1}H NMR (400 Mz, CD_3CN-D_2O (v/v = 1/1), TMS, ppm) δ 0.68 (s, br), 1.07 (s, br), 1.28 (s, br), 1.59 (br), 2.85 (s, br), 2.99 (s, br), 3.24 (dbr), 3.46 (br), 3.53 (br), 3.84 (s, br), 4.23 (br), 4.44 (br), 6.80 (s, br), 7.22 (br), 7.36 (s, br). 7.49 (s, br).

CPT1-B (Yield: 33%) GPC. $M_n = 1.003 \times 10^5$ (PDI = 1.007). ^{1}H NMR (400 Mz, CD_3CN-D_2O (v/v = 1/1), TMS, ppm) δ 0.69 (s, br), 1.08 (s, br), 1.30 (s, br), 1.57−1.68 (dbr), 2.99 (s, br), 3.36 (s, br), 3.54 (s, br), 3.66−3.67 (dbr), 4.03 (br), 4.32 (br), 6.99 (s, br), 7.18 (s, br), 7.34 (s, br).

CPT1-C (Yield: 28%) GPC. $M_n = 1.061 \times 10^5$ (PDI = 1.160). ^{1}H NMR (400 Mz, CD_3CN-D_2O (v/v = 1/1), TMS, ppm) δ 0.68 (s, br), 1.05 (s, br), 1.59 (s, br), 2.85 (s, br), 2.99 (s, br), 3.29 (s, br), 3.50−3.59 (dbr), 4.23 (s, br), 4.45 (s, br), 6.80 (s, br), 7.35 (s, br), 7.49 (s, br).

PT1 (yield: 55.6%) GPC. $M_n = 1.643 \times 10^5$ (PDI = 1.233). ^{1}H NMR (400 Mz, CD_3CN-D_2O (v/v = 1/1), TMS, ppm) δ 1.14 (br), 1.30 (s, br), 1.59−1.69 (dbr), 3.46 (s,br), 4.24 (s, br), 7.21, (s, br).

PT2 (yield: 50.0%) GPC. $M_n = 6.655 \times 10^4$ (PDI = 1.161). ^{1}H NMR (400 Mz, CD_3CN-D_2O (v/v = 1/1), TMS, ppm) δ 0.67−0.69 (br), 1.06 (s,br), 1.60 (s, br), 2.85 (s, br), 3.00 (s, br), 4.56 (s, br), 6.81 (s, br), 7.35−7.37 (dbr), 7.48−7.50 (dbr).

Fluorescent Spectra of CPT1-C with Different Bacteria. Five kinds of freshly diluted bacteria ($C = 10^8$ cfu/mL) were incubated with CPT**1**-C (70 μM, TBS, pH 7.4) for 5 min, and then the bacterial suspensions were used for fluorescence test in a Hitachi F-4500 fluorescence spectrometer with an excitation at 460 nm.

Bacteria Imaging. Fluorescence imaging of bacteria (*E. coli*, *K. pneumoniae*, and *P. aeruginosa*) was performed with an NIKON-SIM confocal laser scanning microscopy using the light source at 561 nm for excitation. A 100-oil-immersion objective lens was used. Freshly diluted *E. coli*, *K. pneumoniae*, and *P.aeruginosa* were cultured in the media in the presence of CPT**1**-C at 70 μM, (TBS buffer solution, pH 7.4). The bacteria were collected by centrifugation at 9,000 rap for 10 min, rinsed with TBS (pH 7.4), and then resuspended in TBS solution (1 mL). The bacteria suspensions were dropped into a cover glass for fluorescence imaging.

■ RESULTS AND DISCUSSION

Molecular Structures of LPS and LTA. LPS and LTA are major constituents of the cell membranes of Gram-negative bacteria and Gram-positive bacteria, respectively. To discriminate the Gram-negative bacteria from Gram-positive bacteria, it is necessary to clearly understand the molecular structures of

Scheme 2. (A) Molecular Structures of LPS, LTA, and sensor CPT1 and (B) Schematic Illustration of the Proposed Interaction Mechanism of CPT1 with LPS Utilizing the Electrostatic Interaction, the Hydrophobic Interaction, and the Conformational Change

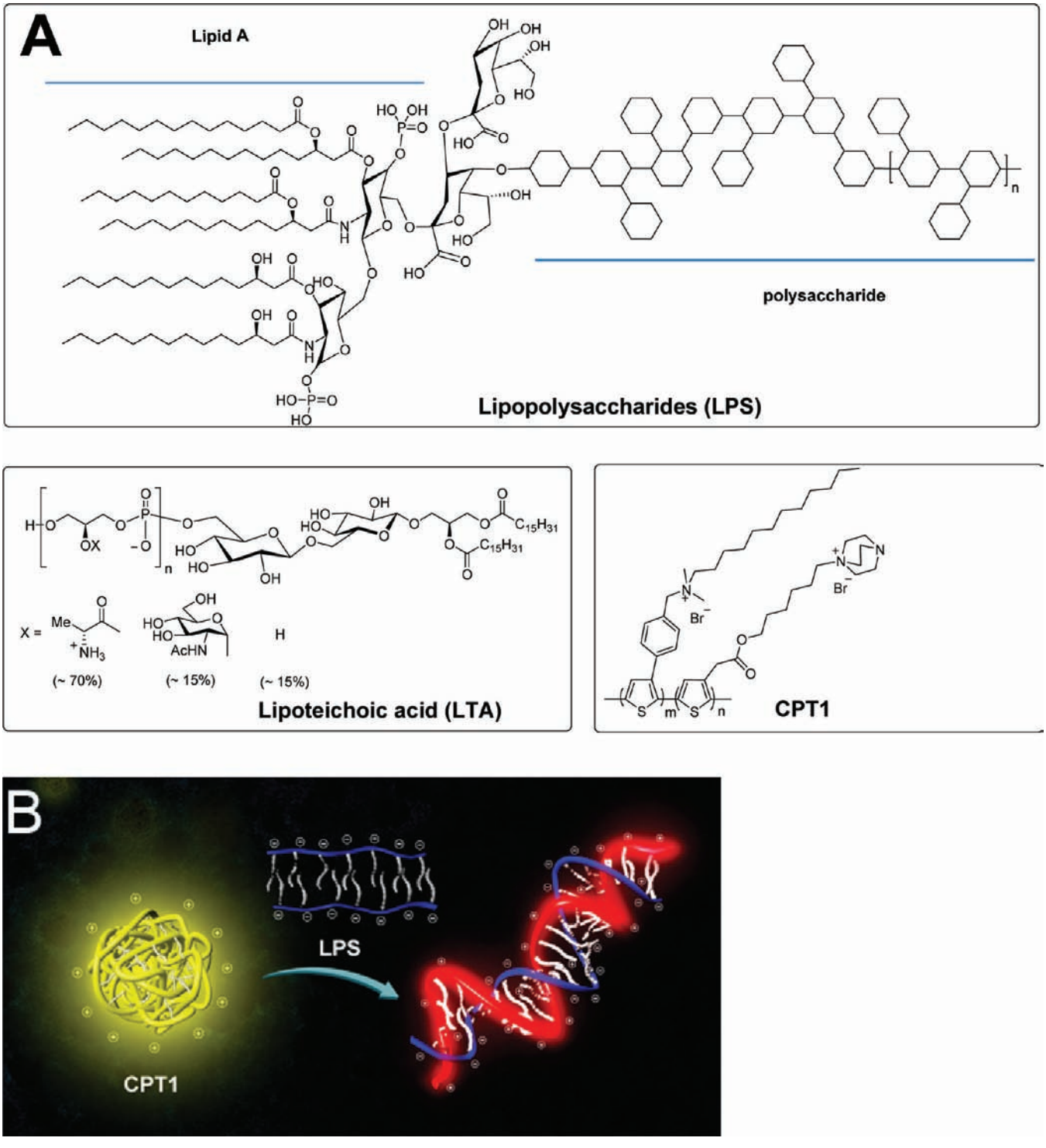

LPS and LTA. As shown in Scheme 2A, the primary toxic component of LPS is the lipid A core which is linked with two 2-keto-3-deoxyoctonate units.[17] LPS is highly negative charged due to the polysaccharide formed with two phosphorylated glucosamine sugars in the lipid A part and two 2-keto-3-deoxyoctonate units. Moreover, six hydrophobic chains in one structural unit make the overall molecule highly amphiphilic. As a result, the highly hydrophobic and negatively charged LPS would automatically arrange in a definite order in aqueous solution. When the concentration of LPS reaches to a certain extent, the phospholipid bilayers will be formed in aqueous solution.[18] In contrast, LTA consists of teichoic acids and long chains of ribitol phosphate, and it is anchored to the lipid bilayer via glyceride. The major difference between LPS and LTA is that over 6 hydrophobic chains exist in one structural

dx.doi.org/10.1021/ja211570a | J. Am. Chem. Soc. 2012, 134, 6685−6694

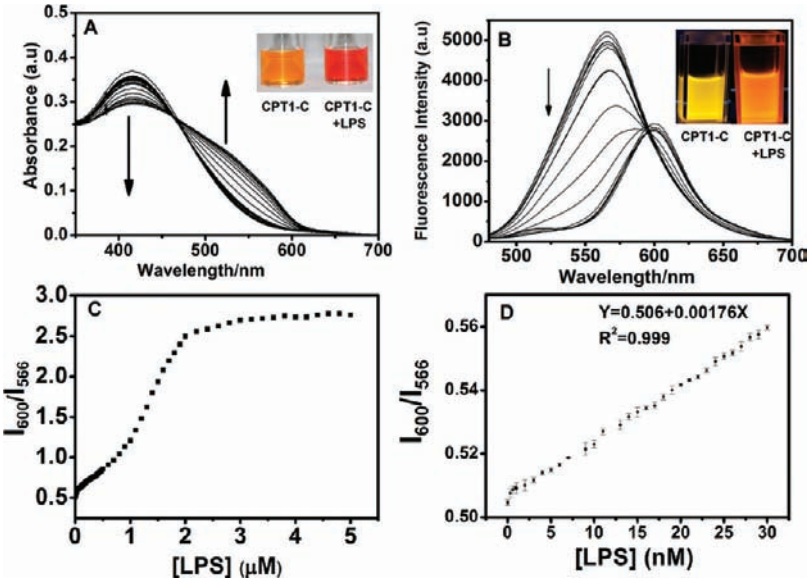

Figure 1. (A) Absorbance titration spectra of CPT**1**-C (50 μM) in 10 mM HEPES buffer solution (1% CH_3CN, pH 7.4) upon gradual addition of LPS from 0 to 5 μM. The inset shows the color change of the resulting solution (0.5 mM CPT**1**-C in the absence and presence of 50 μM LPS). (B) Fluorescence titration spectra of CPT**1**-C upon addition of gradual addition of LPS from 0 to 5 μM with an excitation at 460 nm. The inset shows the corresponding fluorescent color change. The fluorescence intensity ratio (I_{600}/I_{566}) of CPT**1**-C vs the concentrations of LPS (0−5 μM) (C) and (0−30 nM) (D), respectively.

unit of LPS, while only two hydrophobic chains exist in that of LTA.

Design of Copolythiophenes for LPS Detection. Bearing the detailed structural information in mind (vide supra), we designed a water-soluble copolymer (CPT**1**-C) for LPS sensing on the basis of the interactive and complementary interaction. CPT**1**-C is expected to discriminate LPS from LTA, and thus discriminate the Gram-negative bacteria from Gram-positive bacteria. As shown in Scheme 2A, the ammonium and quaternary diazabicyclooctane (DABCO) substituents in CPT**1**-C not only improve its water solubility but also provide two positive centers to bind with the negatively charged LPS *via* electrostatic interaction. In particular, the DABCO moiety has been demonstrated to have a very strong affinity to phosphate groups, as reported in previous work.[16] The ammonium moiety with a C-12 alkyl chain and the DABCO moiety with a C-6 alkyl chain in CPT**1**-C are expected to increase its hydrophobic interaction with LPS in aqueous solution. In addition, the phenyl group introduced to the 3-position of the thiophene ring can be used as a blocking unit to force the polythiophene backbone to adopt a twist conformation.[19] CPT**1**-C will form a quasi-sphere-shaped self-assembly in aqueous solution (vide infra). Upon complexation with LPS, the electrostatic and hydrophobic cooperative interactions between CPT**1**-C and LPS can induce the conformational change of copolythiophene backbone (Scheme 2B). Thus, the steric hindrance from the phenyl group is decreased and the copolythiophene backbone becomes more coplanar. Such a conformational change results in significant red-shifts in both the absorption and fluorescence wavelengths of CPT**1**-C, which has also been observed in other polythiophenes.[20] It should be mentioned that different monomer ratios in the copolymer can be controlled to tune the sensitivity and selectivity to LPS as well.

LPS Sensing with CPT1-C. The interaction between CPT**1**-C (50 μM, calculated on monomers basis) and LPS was studied in HEPES buffer (10 mM, pH 7.4, 1% CH_3CN) at room temperature by absorption and emission spectroscopy. The UV−vis spectrum of CPT**1**-C in HEPES solution displays a characteristic absorption band of polythiophene at 420 nm (Figure 1A). Upon addition of LPS, the absorption peak at 420 nm decreased gradually, a new absorption band at around 540 nm emerged with an isosbestic point at 460 nm, and the color changed from yellow to red. Their corresponding changes in the fluorescence spectra are shown in Figure 1B. In the absence of LPS, CPT**1**-C showed a characteristic polythiophene emission at 566 nm. Upon addition of LPS, the emission peak was red-shifted to 600 nm. Such significant changes in the absorption and fluorescence spectra could be well explained by the LPS-induced conformational change of conjugated backbone through the electrostatic and hydrophobic cooperative interactions between CPT**1**-C and LPS. Particularly, the corresponding effect could be evaluated quantitatively by analyzing the dependence of the fluorescence intensity ratio (I_{600}/I_{566}) on the concentration of LPS. As shown in Figure 1C, the I_{600}/I_{566} ratio increased gradually upon addition of LPS, saturated at [LPS] = 2 μM. Further addition of LPS could not induce obvious changes in the spectrum. By plotting the I_{600}/I_{566} ratio versus the concentration of LPS, a good linear relationship ($I_{600}/I_{566} = 0.506 + 1.76 \times 10^{-3} \times [\mathrm{LPS}]$, $R^2 = 0.999$) was observed for a LPS concentration ranging from 0.3 to 30 nM (Figure 1D). Based on that, the limit of detection (C_{LOD}) was calculated to be 270 pM (Supporting Information),[21,22] which is the lowest value reported thus far (over at least 3 orders of magnitude lower than the literature reports).[5−8]

The zeta-potential analysis was carried out to provide direct evidence for the effective binding of CPT**1**-C with LPS through the electrostatic interaction. The zeta-potential of CPT**1**-C was determined to be +50.2 mV even at low concentration (50 μM), indicating a mass of positive charges on its surface. Upon addition of 5 μM of LPS, the zeta-potential of CPT**1**-C was reduced to −2.12 mV, implying that the negatively charged LPS did interact with CPT**1**-C through the electrostatic interaction.

dx.doi.org/10.1021/ja211570a | J. Am. Chem. Soc. 2012, 134, 6685−6694

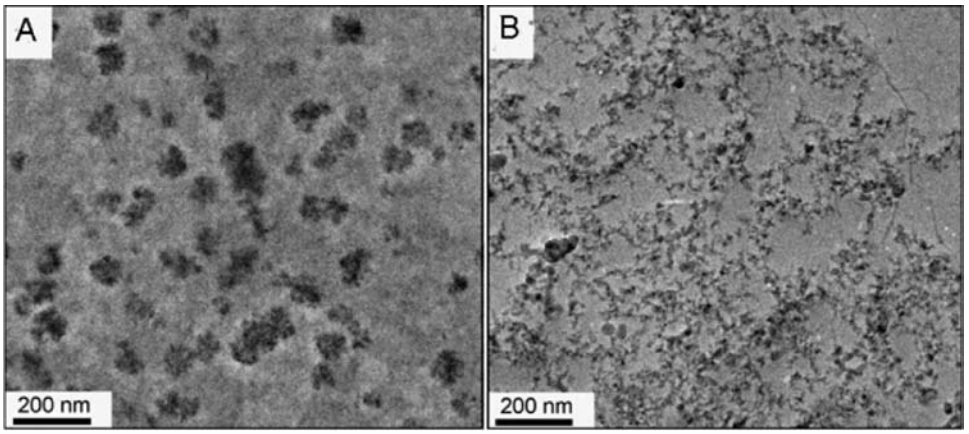

Figure 2. TEM images of CPT**1**-C (50 μM) in 10 mM HEPES buffer solution (1% CH_3CN, pH 7.4) in the absence (A) and presence (B) of 5 μM LPS, respectively.

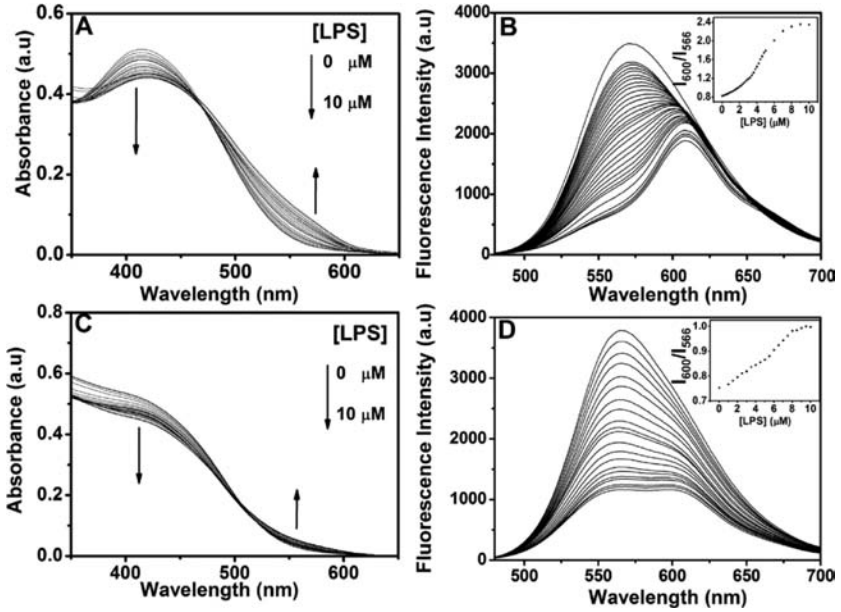

Figure 3. Absorbance and fluorescence titration spectra of CPT**1**-A (A and B) and CPT**1**-B (C and D) (50 μM) in 10 mM HEPES buffer solution (1% CH_3CN, pH 7.4) upon gradual addition of LPS with the concentration ranging from 0 to 10 μM, respectively. The exciting wavelength is 460 nm.

Transmission electron microscopy (TEM, Figure 2) and atomic force microscope (AFM, Figure S1) observations of CPT**1**-C also indicated that the copolymer with long alkyl chains and highly positive charges can form a quasi-sphere-shaped self-assembly in aqueous solution (Figure 2A). The structure was destroyed upon addition of LPS due to the electrostatic and hydrophobic cooperative interactions, and a strong supramolecular complex between LPS and CPT**1**-C with an obvious conformational change was formed (Figure 2B). In addition, the dynamic light scattering studies showed that the mean radius of quasi-sphere-shaped structures of free CPT**1**-C was 118.3 nm, while it increased to 205.3 nm upon addition of LPS (Figure S2), agreeing with TEM and AFM observations. The change of particle structure from quasi-sphere to nonsphere is the major reason for the increase of hydrodynamic radius. Based on these results, it is reasonable to conclude that the conformation of CPT**1**-C is changed from a coil to a more extended structure. The similar conformational change was also observed in homopolythiophenes.[9−11] The above results are well consistent with the spectral changes in Figure 1.

Effect of Different Monomer Ratios in Copolythiophenes. As discussed above, CPT**1**-C can effectively identify LPS in a HEPES buffer solution through the ratiometric changes in absorption and fluorescence spectra. To further illustrate the role of phenyl group at 3-position of thiophene ring in the sensing process, two copolymers (CPT**1**-A and CPT**1**-B) with different monomer ratios (1/1 and 1/2.5, respectively) were prepared. The interaction between CPT**1**-A and LPS was similar to that of CPT**1**-C under the same experimental conditions. For example, CPT**1**-A displayed a characteristic absorption band of polythiophene at 415 nm, and the band shifted to 540 nm with the addition of LPS (Figure 3A). Concomitantly, the emission peak was red-shifted from 566 to 600 nm upon addition of LPS (Figure 3B). The observed color change from yellow to red is believed to be related to a coil-to-rod transition of the conjugated backbone.[19,20] In contrast, CPT**1**-B did not show a significant

dx.doi.org/10.1021/ja211570a | J. Am. Chem. Soc. 2012, 134, 6685−6694

change in the absorption spectra upon addition of LPS (Figure 3C) due to fewer amount of rigid phenyl groups in the copolymer chain, and the corresponding fluorescence spectra displayed less ratiometric changes (Figure 3D).

To further compare the sensitivity of three copolymers to LPS, we defined the signal-to-background ratio (S/B) using the following equation:[22]

$$S/B = (I_{600}/I_{566})_{withLPS}/(I_{600}/I_{566})_{withoutLPS}$$

where $(I_{600}/I_{566})_{withLPS}$ and $(I_{600}/I_{566})_{withoutLPS}$ represent the I_{600}/I_{566} ratios in the presence and absence of LPS, respectively. It was found that the monomer ratios of three copolymers calculated from the integrity area were associated with the mole ratio of two added monomers and would signaly affect the S/B value. As shown in Table 1, the signal-to-background ratio of CPT**1**-C with 2.5/1 mol ratio is up to 5.453, which is much higher than those of CPT**1**-A (1.945, 1/1) and CPT**1**-B (1.135, 1/2.5). The results coincide well with the spectral changes of the copolythiophenes.

Table 1. Comparable Data of Three Copolythiophenes to LPS

	CPT1-A	CPT1-B	CPT1-C
monomer **4**/monomer **2**[a]	1/1	1/2.5	2.5/1
monomer **4**/monomer **2**[b]	1.07/1	1/2	5/1
$(I_{600}/I_{566})_{withoutLPS}$[c]	0.825	0.753	0.51
$(I_{600}/I_{566})_{withLPS}$[c]	1.605	0.855	2.781
S/B[d]	1.945	1.135	5.453

[a]The mole ratio obtained from the added monomers. [b]The mole ratio calculated from the integrity in ^{1}H NMR spectrum (Supporting Information). [c]The ratio of the fluorescence intensity at 600 and 566 nm in the absence and presence of LPS (4.5 μM), respectively. [d]The signal-to-background ratio (S/B) of three copolythiophenes to LPS.

Interaction between Two Homopolythiophenes and LPS. To verify that it is indeed the cooperative interaction leading to the high snsitivity of CPT**1**-C to LPS, two corresponding homopolythiophenes were prepared as model polymers (PT**1** and PT**2**) for comparison. PT**1** contains a C-6 alkyl chain with DABCO terminal, while PT**2** contains a phenyl and an ammonium with C-12 alkyl terminal. As depicted in Figure 4B, PT**1** showed a characteristic polythiophene emission at 550 nm in the absence of LPS. Upon addition of LPS, the fluorescence intensity at 550 nm was monotonously decreased and the peak location maintained until the concentration of LPS reached 4.5 μM. Meanwhile, there was a slight blue shift in the absorption spectroscopy (Figure 4A). The nonregioregular polythiophene derivative is considered to allow only the formation of weak and localized conformation defects along the backbone, leading to a continuous and monotonic decrease of the fluorescence intensity upon complexation with analytes.[23] PT**2** is not able to interact effectively with LPS through the electrostatic interaction because it lacks the DABCO group to bind with the phosphate groups. In addition, the structure with only one long chain also decreases its hydrophobic interaction with LPS. As a result, the addition of LPS results in smaller red-shifts both in the absorption and fluorescence wavelengths of PT**2** (Figure 4D). These results strongly support the suggestion that the cooperative and complementary interaction can play essential role in the molecular design, and each functional substituent in CPT**1**-C is indispensable for highly sensitive detection of LPS.

Reactivity of CPT1-C with Other Biologically Important Species. Selectivity is another essential parameter for the practical application of CPT**1**-C. The selectivity of the sensor for LPS was evaluated by the fluorescence intensity ratio (I_{600}/I_{566}) response in the presence of various biologically important species in buffer solution. As illustrated in Figure 5, nearly all of the other biological molecules (except for LTA) do not give rise to significant increase in I_{600}/I_{566} ratio. LTA and LPS have closely similar molecular structures; both of them contain phosphates and long hydrophobic chains. LPS is higher negative charged and more hydrophobic than LTA. However, only LPS could induce change in the fluorescence intensity ratio (I_{600}/I_{566}) by at least a factor of 3. The addition of LTA gave rise to a less signal response compared to that of LPS. The

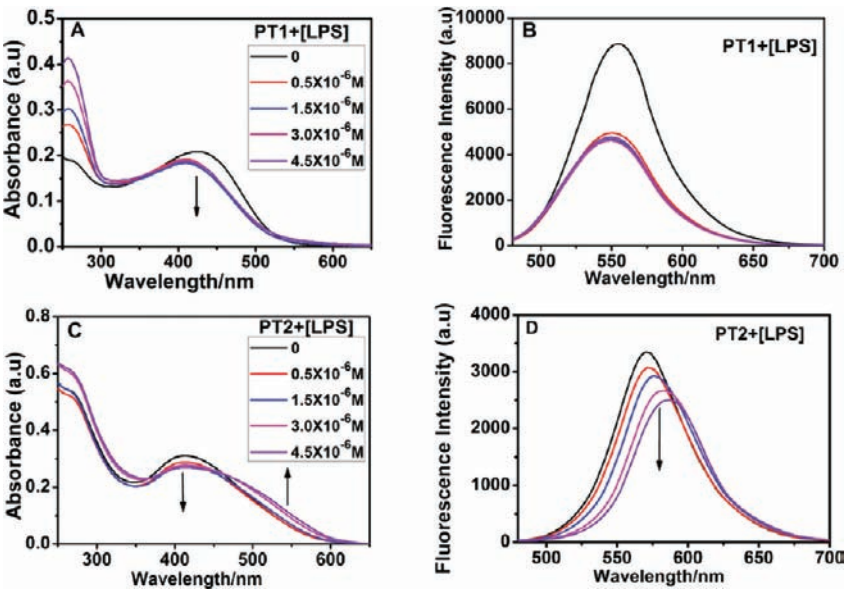

Figure 4. Absorbance and fluorescence titration spectra of PT**1** (A and B) and PT**2** (C and D) (50 μM) in 10 mM HEPES buffer solution (1% CH_3CN, pH 7.4) upon gradual addition of LPS with the concentration ranging from 0 to 4.5 μM. The exciting wavelength is 460 nm.

dx.doi.org/10.1021/ja211570a | J. Am. Chem. Soc. 2012, 134, 6685−6694

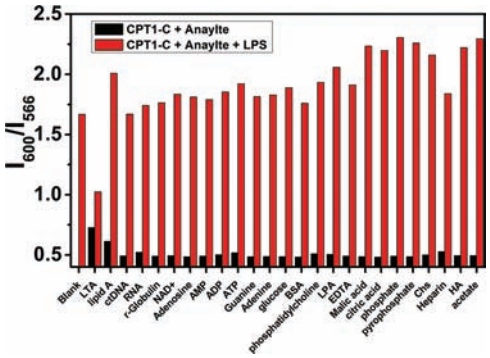

Figure 5. Selectivity of CPT**1**-C (50 μM) to LPS (1.2 μM) in 10 mM HEPES buffer solution (1% CH_3CN, pH 7.4) in the presence of some coexisting biological species including lipoteichoic acid (LTA), lipid A, ctDNA, RNA, γ-globulins, NAD^+, adenosine, AMP, ADP, ATP, guanine, adenine, glucose, BSA, Phosphatidylcholine, LPA, EDTA, malic acid, citric acid, phosphate, pyrophosphate, chondroitin 4-sulfate sodium salt (Chs), heparin, hyaluronic acid (HA), acetate. ctDNA, RNA, γ-globulins, and BSA were 1 mg/L, LTA was 1.2 μM, and the other anions or biological molecules were 2 μM. Blank refers to free CPT**1**-C solution. Black pillars and red pillars refer to these analytes in the absence and presence of 1.2 μM LPS, respectively.

observation can be simply explained by the fact that a biological species having only a single alkyl chain or a low negative charge density cannot effectively bind with CPT**1**-C and cause significant conformational changes. In contrast, CPT**1**-C interacts with LPS by the multiple electrostatic and hydrophobic cooperative interactions, which results in a distinct conformational change. Concomitantly, the UV−vis absorption spectra of CPT**1**-C also varied significantly only in the presence of LPS and induced obvious color change (Figure S3). It was revealed that the lipid A itself only led to a slight increase in the fluorescence intensity ratio (I_{600}/I_{566}) compared with LPS (Figure 5). The reason could probably be attributed to more electrostatic interaction sites (i.e., carboxyl) between LPS and CPT1-C than that of lipid A itself in comparison of the molecular structures of LPS with lipid A. Furthermore, CPT**1**-C shows a distinct signaling increase to LPS in the presence of the coexisting lipid A, demonstrating that CPT1-C has a superior selectivity to LPS over lipid A. The results indicate that the colorimetric and fluorometric sensor is highly selective to LPS even in the presence of biologically competing species.

pH-Dependent Response. To further study the practical applicability of this sensor, the pH effects of CPT**1**-C in the presence of LPS were also investigated. Experimental results indicated that the fluorescence intensity ratio (I_{600}/I_{566}) of CPT**1**-C did not change obviously in a wide pH range from 4 to 11 (Figure 6). Upon addition of LPS, this intensity ratio showed enhancements by about a factor of 3 and a distinct platform between pH 4 and 11, demonstrating that CPT**1**-C can be used to detect LPS throughout a wide pH range.

Discrimination of Gram-Negative Bacteria from Gram-Positive Bacteria. Bacterial contamination is a major health hazard especially in the context of food safety, environmental monitoring, and the pharmaceutical industry. Thus, rapid differentiation of bacteria is imperative for clinical diagnosis, food safety and therapeutic strategies. Gram staining is a conventional method to differentiate bacterial species from Gram-positive bacteria and Gram-negative bacteria based on the distinct chemical and physical properties of their cell walls. Gram-positive bacteria are stained dark blue or violet by Gram

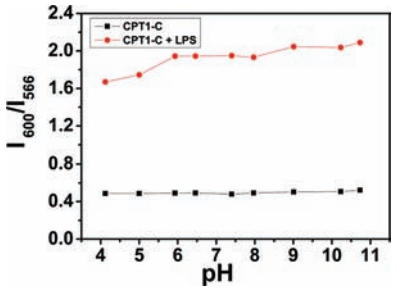

Figure 6. Effect of pH on the fluorescence intensity ratio (I_{600}/I_{566}) of free CPT**1**-C (50 μM) (black squares) and CPT**1**-C/LPS (1.5 μM) mixtures (red dots) at room temperature.

staining, while Gram-negative bacteria, which cannot retain the crystal violet stain, instead take up the counter-stain and appear in red or pink.[24] However, this method requires numerous tedious procedures including pretreatment in harsh conditions. Because LPS is the main constituent of the outer membrane of Gram-negative bacteria and CPT**1**-C is highly selective and sensitive to LPS, CPT1-C is thus expected to be able to distinguish Gram-negative bacteria and Gram-positive bacteria. In this work, three kinds of Gram-negative bacteria (*E. coli*, *K. pneumoniae*, and *P. aeruginosa*) and two kinds of Gram-positive bacteria (S. epidermidis and S. aureus) were used as example targets. Freshly diluted bacteria (C = 10^8 cfu/mL) were incubated with CPT**1**-C (70 μM, TBS, pH 7.4) for 5 min, and then the bacterial suspensions were used for fluorescence test in a Hitachi F-4500 fluorescence spectrometer with an excitation at 460 nm. Figure 7A shows the photo- and fluorescent-images of five kinds of bacteria after incubation with CPT**1**-C. Gram-positive bacteria incubating with CPT**1**-C induced a colorless solution (2 and 3) and the fluorescence was quenched. In

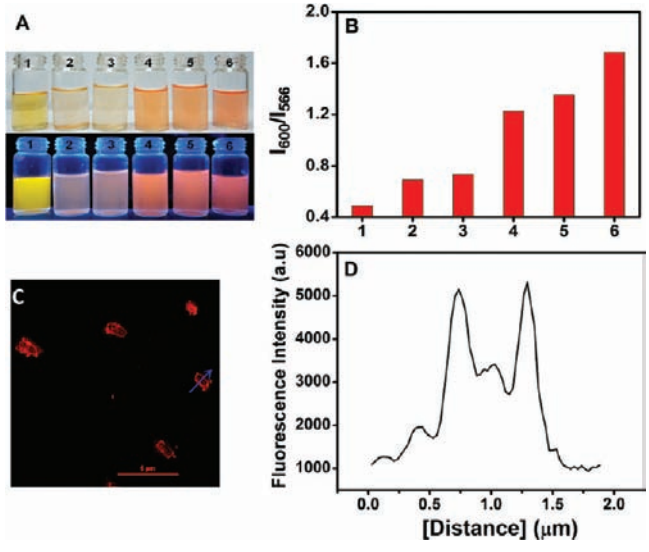

Figure 7. (A) Photoimages and fluorescent-images for five kinds of bacteria (10^8 cfu/mL) after incubation with CPT**1**-C for 5 min. The numbers 1, 2, 3, 4, 5, 6 refer to free CPT**1**-C, *S. aureus*, *S. epidermidis*, *E. coli*, *K. pneumoniae*, and *P. aeruginosa* incubate in CPT**1**-C solution, respectively. (B) Fluorescence intensity ratio (I_{600}/I_{566}) vs five kinds of bacteria (10^8 cfu/mL) after incubated with CPT**1**-C (70 μM). (C) Confocal fluorescence image of *E. coli* (10^8 cfu/mL) after incubation with CPT**1**-C in fresh medium solution (λ_{ex} = 561 nm). (D) The fluorescence intensity profile across the line is shown in (C).

dx.doi.org/10.1021/ja211570a | *J. Am. Chem. Soc.* 2012, 134, 6685−6694

contrast, the Gram-negative bacteria which contain LPS showed a visual color change from yellow to orange and the fluorescence color changed from yellow to pink. The observations are also consistent with the fluorescent spectra obtain from five kinds of bacteria after incubation with CPT**1**-C (Figure 7B). These results demonstrate that CPT**1**-C as a dual colorimetric and fluorometric sensor for LPS is able to rapidly distinguish Gram-negative bacteria from Gram-positive bacteria, which is very important and useful for practical application. In order to demonstrate directly whether the sensor is also capable of interacting with LPS on the surface of bacteria, fluorescence imaging of bacteria (*E. coli*, *K. pneumoniae*, and *P. aeruginosa*) after incubated with CPT**1**-C was performed with an NIKON-SIM confocal laser scanning microscopy. As shown in Figure 7C, a strong red fluorescence was observed outside the cells and the fluorescence intensity of the outside cells was stronger than that of the middle (Figure 7D). Similar results were also obtained on *K. pneumoniae* and *P. aeruginosa* after incubation with CPT**1**-C (Figure S4), confirming that CPT**1**-C is capable of interacting with LPS on the surface of bacteria.

■ CONCLUSIONS

In summary, we developed for the first time a copolythiophene CPT**1**-C to function as a colorimetric and fluorometric sensor with an ultrahigh sensitivity at the picomolar level toward LPS in aqueous solution, which is by 3 orders of magnitude lower than the most recently reported LPS sensors. To the best of our knowledge, the CPT**1**-C sensor shows the lowest detection limit among all synthetic LPS probes reported so far. The sensor is also highly selective toward LPS in the presence of other negatively charged analytes coexisting with LPS, and the excellent selectivity has been illustrated to be due to the multiple electrostatic and hydrophobic cooperative interactions. As a practical example, we also demonstrate that CPT**1**-C is able to distinguish Gram-negative bacteria from Gram-positive bacteria even upon on visual observation. We believe that the newly proposed design strategy based on the copolymerization method can also be extended to design other sensors for highly sensitive and selective sensing of various biologically important polyanions.

■ ASSOCIATED CONTENT

Supporting Information

Details of the syntheses, spectroscopic characterization, UV–vis spectra, DLS and AFM experiments, the calculation of the limit of detection, confocal fluorescence imaging of *K. pneumoniae* and *P. aeruginosa* after incubation with CPT**1**-C. This material is available free of charge via the Internet at http://pubs.acs.org.

■ AUTHOR INFORMATION

Corresponding Author

wangpf@mail.ipc.ac.cn; apwjzh@cityu.edu.hk

Notes

The authors declare no competing financial interest.

■ ACKNOWLEDGMENTS

M.L. thanks Engineers Jianchun Zhou and Zhihong Xue (Nikon Instruments (Shanghai) Co. LTD. Beijing Branch) for help with the confocal fluorescence imaging. This work was supported by the NNSF of China (Grant Nos. 21073213, 60978034 and 20903110), the Main Direction Program of Knowledge Innovation of Chinese Academy of Sciences, and the National High Technology Research and Development Program of China (863 Program; Grant No. 2009AA03Z318).

■ REFERENCES

(1) (a) Young, L. S.; Martin, W. J.; Meyer, R. D.; Weinstein, R. J.; Anderson, E. T. *Ann. Intern. Med.* **1977**, *86*, 456–471. (b) Ulevitch, R. J. *Adv. Immunol.* **1993**, *53*, 267–289. (c) Ulevitch, R. J.; Tobias, P. S. *Curr. Opin. Immunol.* **1994**, *6*, 125–130. (d) Seltmann, G.; Holst, O. *The Bacterial Cell Wall*; Springer: New York, 2002.

(2) (a) Beutler, B.; Rietschel, E. T. *Nat. Rev. Immunol.* **2003**, *3*, 169–176. (b) Warren, H. S.; Fitting, C.; Hoff, E.; Adib-Conquy, M.; Beasley-Topliffe, L.; Tesini, B.; Liang, X.; Valentine, C.; Hellman, J.; Hayden, D.; Cavaillon, J. M. *J. Infect. Dis.* **2010**, *201*, 223–232.

(3) (a) Raetz, C. R. H. *Annu. Rev. Biochem.* **1990**, *59*, 129–170. (b) Van Amersfoort, E. S.; Van Berkel, T. J. C.; Kuiper, J. *Clin. Microbiol. Rev.* **2003**, *16*, 379–414.

(4) (a) Roslansky, P. F.; Novitsky, T. J. *J. Clin. Microbiol.* **1991**, *29*, 2477–2483. (b) Zhang, G.; Baek, L.; Nielsen, P. E.; Buchardt, O.; Koch, C. *J. Clin. Microbiol.* **1994**, *32*, 416–422.

(5) Rangin, M.; Basu, A. *J. Am. Chem. Soc.* **2004**, *126*, 5038–5039.

(6) Voss, S.; Fischer, R.; Jung, G.; Wiesmüller, K. H.; Brock, R. *J. Am. Chem. Soc.* **2007**, *129*, 554–561.

(7) Wu, J.; Zawistowski, A.; Ehrmann, M.; Yi, T.; Schmuck, C. *J. Am. Chem. Soc.* **2011**, *133*, 9720–9723.

(8) (a) Rustici, A.; Velucchi, M.; Faggioni, R.; Sironi, M.; Ghezzi, P.; Quataert, S.; Green, B.; Porro, M. *Science* **1993**, *259*, 361–365. (b) Li, C.; Budge, L. P.; Driscoll, C. D.; Willardson, B. M.; Allman, G. W.; Savage, P. B. *J. Am. Chem. Soc.* **1999**, *121*, 931–940. (c) Chan, S.; Horner, S. R.; Fauchet, P. M.; Miller, B. L. *J. Am. Chem. Soc.* **2001**, *123*, 11797–11798. (d) Hubbard, R. D.; Horner, S. R.; Miller, B. L. *J. Am. Chem. Soc.* **2001**, *123*, 5810–5811. (e) Ganesh, V.; Bodewits, K.; Bartholdson, S. J.; Natale, D.; Campopiano, D. J.; Mareque-Rivas, J. C. *Angew. Chem., Int. Ed.* **2009**, *48*, 356–360.

(9) (a) Nilsson, K. P. R; Inganäs, O. *Nat. Mater.* **2003**, *2*, 419–424. (b) Ho, H. A.; Najari, A.; Leclerc, M. *Acc. Chem. Res.* **2008**, *41*, 168–178.

(10) Ho, H. A.; Béra-Abérem, M.; Leclerc, M. *Chem.—Eur. J.* **2005**, *11*, 1718–1724.

(11) (a) Li, C.; Numata, M.; Takeuchi, M.; Shinkai, S. *Angew. Chem., Int. Ed.* **2005**, *44*, 6371–6374. (b) Li, C.; Numata, M.; Takeuchi, M.; Shinkai, S. *Chem. Asian J.* **2006**, *1*, 95–101. (c) Yao, Z.; Li, C.; Shi, G. *Langmuir* **2008**, *24*, 12829–12835. (d) Yao, Z.; Feng, X.; Hong, W.; Li, C.; Shi, G. *Chem. Commun.* **2009**, 4696–4698.

(12) (a) Zhou, Q.; Swager, T. M. *J. Am. Chem. Soc.* **1995**, *117*, 12593–12602. (b) Swager, T. M. *Acc. Chem. Res.* **1998**, *31*, 201–207. (c) Heeger, P. S.; Heeger, A. J. *Proc. Natl. Acad. Sci. U.S.A.* **1999**, *96*, 12219–12221. (d) McQuade, D. T.; Pullen, A. E.; Swager, T. M. *Chem. Rev.* **2000**, *100*, 2537–2574. (e) Thomas, S. W.; Joly, G. D.; Swager, T. M. *Chem. Rev.* **2007**, *107*, 1339–1386. (f) Lee, K.; Povlich, L. K.; Kim, J. *Analyst* **2010**, *135*, 2179–2189.

(13) (a) Petrak, K. *Polyelectrolytes: Science and Technology*; Marcel Dekker: New York, 1992; pp 265–297. (b) Song, Y.; Wei, W.; Qu, X. *Adv. Mater.* **2011**, *23*, 4215–4236.

(14) (a) Tyagi, S.; Kramer, F. R. *Nat. Biotechnol.* **1996**, *14*, 303–308. (b) Yang, C. J.; Jockusch, S.; Vicens, M.; Turro, N. J.; Tan, W. *Proc. Natl. Acad. Sci. U.S.A.* **2005**, *102*, 17278–17283. (c) Han, Z.; Zhang, X.; Zhou, L.; Gong, Y.; Wu, X.; Zhen, J.; He, C.; Jian, L.; Jing, Z.; Shen, G.; Yu, R. *Anal. Chem.* **2010**, *82*, 3108–3113.

(15) (a) Zeng, L.; Wu, J.; Dai, Q.; Liu, W.; Wang, P.; Lee, C. S. *Org. Lett.* **2010**, *12*, 4014–4017. (b) Zeng, L.; Liu, W.; Zhuang, X.; Wu, J.; Wang, P.; Zhang, W. *Chem. Commun.* **2010**, *46*, 2435–2437. (c) Dai, Q.; Liu, W.; Zhuang, X.; Wu, J.; Zhang, H.; Wang, P. *Anal. Chem.* **2011**, *83*, 6559–6564. (d) Wu, J.; Liu, W.; Ge, J.; Zhang, H.; Wang, P. *Chem. Soc. Rev.* **2011**, *40*, 3483–3495.

(16) (a) Tabushi, I.; Imuta, J. I.; Seko, N.; Kobuke, Y. *J. Am. Chem. Soc.* **1978**, *100*, 6287–6288. (b) Giwa, C. O.; Hudson, M. J.; Morenoreal, L.; Rodriguez-Castellon, E. *J. Chem. Soc. Chem. Commun.*

1987, 536−537. (c) Li, H.; Wang, P.; Wu, S. *Acta Chim. Sinica* **1999**, *57*, 149−154. (d) Singh, R.; J. D., Jr; Dutta, P. K. *Micropor. Mesopor. Mat.* **2004**, *71*, 149−155.
(17) (a) Shands, J. W. *Infec. Immun.* **1971**, *4*, 167−172. (b) Morath, S.; von Aulock, S.; Hartung, T. *J. Endotoxin Res.* **2005**, *11*, 348−356.
(18) Snyder, S.; Kim, D.; McIntosh, T. J. *Biochemistry* **1999**, *38*, 10758−10767.
(19) (a) Lévesque, I.; Leclerc, M. *J. Chem. Soc. Chem. Commun.* **1995**, 2293−2294. (b) Faïd, K.; Leclerc, M. *Chem. Commun.* **1996**, 2761−2762. (c) Chayer, M.; Faïd, K.; Leclerc, M. *Chem. Mater.* **1997**, *9*, 2902−2905.
(20) Feng, X.; Liu, L.; Wang, S.; Zhu, D. *Chem. Soc. Rev.* **2010**, *39*, 2411−2419.
(21) Zheng, J.; Li, J.; Gao, X.; Jin, J.; Wang, K.; Tan, W.; Yang, R. *Anal. Chem.* **2010**, *82*, 3914−3921.
(22) Huang, J.; Zhu, Z.; Bamrungsap, S.; Zhu, G.; You, M.; He, X.; Wang, K.; Tan, W. *Anal. Chem.* **2010**, *82*, 10158−10163.
(23) Xue, C.; Cai, F.; Liu, H. *Chem.—Eur. J.* **2008**, *14*, 1648−1653.
(24) (a) Dolley, C. D. *The Technology of Bacteria Investigation; explicit directions for the study of bacteria: their culture, staining, mounting, etc.*; S. E. Cassino and Company: Boston, 1885. (b) Bergey, D. H.; John, G. H.; Noel, R. K.; Peter, H. A. S. *Bergey's Manual of Determinative Bacteriology*, 9th ed.; Lippincott Williams & Wilkins: New York, 1994.